Journal of Neuroscience Methods 172 (2008) 131–136

Contents lists available at ScienceDirect

Journal of Neuroscience Methods

journal homepage: www.elsevier.com/locate/jneumeth

Long-range correlation of renal sympathetic nerve activity in both conscious and anesthetized rats

Li Yatang[a], Qiu Jiaheng[a], Yang Zhuo[b], Edward J. Johns[c], Zhang Tao[a,*]

[a] Key Laboratory of Bioactive Materials, Ministry of Education and the College of Life Sciences, Nankai University, Tianjin 300071, PR China
[b] College of Medicine Science, Nankai University, Tianjin 300071, PR China
[c] Department of Physiology, University College of Cork, Cork, Ireland

ARTICLE INFO

Article history:
Received 29 January 2008
Received in revised form 12 April 2008
Accepted 16 April 2008

Keywords:
Anesthesia
Fractal
Long-range correlation
Multiscale entropy
Detrended fluctuation analysis
Renal sympathetic nerve activity

ABSTRACT

In this study we employed both detrended fluctuation analysis (DFA) and multiscale entropy (MSE) measurements to compare the long-range temporal correlation (LRTC) of multifibre renal sympathetic nerve activity (RSNA) between conscious and anesthetized Wistar rats. It was found that both methods showed the obvious LRTC properties in conscious state. Moreover, the scaling exponent of the RSNA in conscious rats was significantly higher than that in anesthetized rats. The results of MSE analysis showed that the entropy values, derived from the conscious group, increased on small time scales and then stabilized to a relatively constant value whereas the entropy measure, derived from anesthetized animals, almost monotonically decreased. This suggests that the fractal properties of underlying dynamics of the system have been reduced by anesthesia. The results demonstrate that apparently random fluctuations in multifibre RSNA are dictated by a complex deterministic process that imparts "long-term" memory to the dynamic system. However, this memory is significantly weakened by anesthesia.

1. Introduction

Activity within the sympathetic nerves to the kidney is largely determined by integration of sensory information within the hypothalamic areas of the brain of sensory information (Zhang and Johns, 1998). Examining how the brain does this is difficult at the single unit level, but one approach is to study the pattern of activity within multifibre recordings making up the signals of renal sympathetic nerve activity (RSNA). It has become apparent that the impact of RSNA on kidney function may not be determined solely by the absolute level of activity within the nerve signal, but more by how the pattern of the energy is distributed across the signal and how it changes dynamically (Stauss et al., 1997; Zhang et al., 1997, 2007; Malpas et al., 1998). In an attempt to address this issue, a number of investigations have applied mathematical methods to measure patterns of activity and one of the most developed approaches is power spectral analysis. Studies in experimental animals have revealed that, in the renal sympathetic nerve, major energy peaks occur at heart rate frequency, respiratory frequency and also at much lower frequencies (Persson et al., 1992; Malpas et al., 1998; Burgess et al., 1999; Yang et al., 2002).

Frequency domain analysis, based on fast Fourier transform (FFT), fails to provide helpful information related to nonlinear characteristics of RSNA, especially for detecting any nonlinear changes of the underlying network, which may be activated. Since multifibre RSNA may represent a nonlinear dynamical system with high dimension, in a previous study, a technique called cluster method was developed whereby nonlinear dynamic analysis could be applied to a complex signal, specifically multifibre recordings of renal nerve activity (Malpas and Ninomiya, 1992). We were able to extract an important variable from the raw renal neurogram, which was simple and had a low dimension, making it suitable for nonlinear analysis. This approach has been applied in various physiological and pharmacological challenges (Zhang and Johns, 1998; DiBona et al., 2000; DiBona and Jones, 2001; Trzebski et al., 2001; Li et al., 2006). However, since the cluster method, which was used to extract the cardiac-related bursts, is actually only suitable to identify rhythms above the respiratory frequency (Malpas, 1998), some information is inevitably neglected by using this measure.

Moreover, most quantitative approaches for analyzing the temporal dynamics of RSNA, including power spectral analysis in frequency domain and nonlinear dynamical methods, require the RSNA signal to be stationary, that is, the signal mean, variance do not change with time (Parish et al., 2004). While RSNA signals might remain stationary for a few seconds at a time, stationarity often fluctuates over very short epochs, limiting the usefulness of

* Corresponding author. Tel.: +86 22 23500237; fax: +86 22 23508800.
E-mail address: zhangtao@nankai.edu.cn (T. Zhang).

0165-0270/$ – see front matter © 2008 Elsevier B.V. All rights reserved.
doi:10.1016/j.jneumeth.2008.04.015

these methods for investigating long-range temporal correlation (LRTC).

New mathematical algorithms have been developed recently to make the problem of analyzing LRTC in non-stationary data tractable. Detrended fluctuation analysis (DFA) (Peng et al., 1992) is one such algorithm. This is a scaling analysis method that provides a simple quantitative parameter to represent the correlation properties in non-stationary time series. Detrending the signal on multiple time scales has been demonstrated to eliminate spurious detection of temporal correlations that arise as an artifact of non-stationarity, thus allowing the method to determine a scaling exponent that characterizes the temporal correlations in monofractal signals (Peng et al., 1992). Recently, DFA has been applied to various physiological signals, including EEG (Linkenkaer-Hansen et al., 2001; Parish et al., 2004; Nikulin and Brismar, 2005; Gifani et al., 2007), signal neuron discharge (Bhattacharya et al., 2005), heart rate (Bunde et al., 2000; Ashkenazy et al., 2001) and human gait (Hausdorff et al., 1995). Another new technique, multiscale entropy (MSE) (Costa et al., 2002) derived from sample entropy (SampEn) (Richman and Moorman, 2000), was recently introduced as a better method to evaluate the complexity of time series. SampEn is based upon single-scale analysis and it does not fully take into account the complex temporal fluctuations inherent in physiological control systems. Because fractal properties have been found in many biological systems including cardiovascular system, a meaningful measure of complexity should take into account multiple time scales (Costa et al., 2005b). Recently, MSE has been employed as a powerful tool to analyze various physiological time series (Costa et al., 2005a; Nikulin and Brismar, 2005; Bornas et al., 2006; Escudero et al., 2006).

The effects of anesthesia on RSNA have been extensively investigated in animals anesthetized with pentobarbital sodium (Iriki and Kozawa, 1983; Morita et al., 1987), chloralose and urethane (Matsukawa and Ninomiya, 1989). Previous studies have demonstrated that chloralose anesthesia caused a marked increase in RSNA, whereas urethane decreased RSNA significantly (Matsukawa and Ninomiya, 1989). In order to diminish the effect of anesthesia on the amplitude of RSNA, a mixture of chloralose and urethane has been widely employed in animal experiments (Zhang et al., 2007). However, how the fractal properties change after anesthesia was unknown. To the best of our knowledge, both DFA and MSE have not been used in any studies on LRTC of RSNA signals. In the present study, we introduced both DFA and MSE to examine the pattern of RSNA and addressed the issue as to whether the LRTC of multifibre RSNA exists and could be detected by these two measures. Furthermore, we examined the hypothesis that the DFA and MSE analysis of RSNA would reveal difference in the LRTC between rats anesthetized with a mixture of chloralose and urethane and conscious animals, which has not been achieved as yet using other complex analysis approaches.

2. Methods

The experiments were approved by the local ethical committee of the University College Cork and the University of Nankai.

2.1. Animal experiments

2.1.1. Anesthetized group

The experiments were performed on 15 male rats (Wistar), 300 ± 6 g, anesthetized with a mixture of urethane/chloralose (650 mg/kg, 50 mg/kg, respectively) given i.v. after initial induction with Enflurane. An adequate depth of anesthesia was monitored by observing arterial blood pressure, heart rate and the absence of corneal and paw-pinch reflexes, and was maintained by regular 1 h administration of additional anesthetic (i.v.) or sooner if needed. The femoral artery was cannulated and connected to a pressure transducer for continuous recording of arterial blood pressure. The left kidney was exposed retroperitoneally and a branch of the nerve to the kidney was placed on a bipolar electrode. Blood pressure was measured. Renal sympathetic nerve activity was amplified with a gain of 100,000 and filtered by high- and low-pass filters set at 0.2 kHz and 2 kHz. The signals were digitized with a sampling frequency of 1000 Hz and displayed on an oscilloscope and stored for later analysis. The neural signals were sampled for 164 s.

2.1.2. Conscious group

The experiments were performed on 15 male rats (Wistar), 285 ± 6 g, under aseptic conditions. The rats were deeply anesthetized with sodium pentobarbital, 60 mg/kg, i.p. and the right carotid artery was cannulated and the cannula was taken subcutaneously to exit between the ears. Using a flank incision, the renal sympathetic nerves were isolated, placed on bipolar recording electrodes and sealed into place with Wacker silgel 932 and, via a subcutaneous route, the recording electrodes were tunnelled to exit between the ears (Huang et al., 2006). The rats were then allowed to recover from anesthesia and signs of post-operative pain controlled by subcutaneous analgesic (buprenorphine 0.1 ml/100 g). Experiments were not begun earlier than 3 days after surgery. The cannula and recording electrodes were attached to a tethering mechanism containing a swivel device which allowed the animal to move freely within its home cage. Blood pressure was measured. Renal sympathetic nerve activity was amplified with a gain of 100,000 and filtered by high- and low-pass filters set at 0.2 kHz and 2 kHz. The signals were digitized with a sampling frequency of 1000 Hz and displayed on an oscilloscope and stored for later analysis. The neural signals were sampled for 164 s.

2.2. Detrended fluctuation analysis

DFA is a scaling analysis method that can be used to investigate the long-range correlation properties in noisy non-stationary time sequences (Peng et al., 1992). The DFA procedure consists of four steps, and was performed as follows. First, the profile is defined as $Y(i) = \sum_{k=1}^{i} x_k - \langle x \rangle$, where $i = 1, 2, 3, \ldots, N$ and $\langle x \rangle$ is the mean RSNA. The integrated signal $Y(i)$ was then divided into $N_s = \mathrm{int}(N/n)$ non-overlapping windows of size s. Since generally the length N was not a multiple of s, a short part at the end of the profile remained in most cases. In order to include this part, the similar procedure was repeated from the opposite direction. Thus, $2N_s$ windows were obtained altogether (Kantelhardt et al., 2001). Subsequently, for each windows, the local linear trend was calculated by least-squares fit, and then the variance for each of $2N_s$ is determined:

$$F_s^2(v) = \frac{1}{s}\sum_{i=1}^{s}(Y(i) - p_v(i))^2 \quad (1)$$

where $p_v(i)$ is the fitting polynomial in the vth windows, $v = 1, 2, 3, \ldots, 2N_s$. Finally, the square root of the average over all windows was taken to compute the fluctuation function:

$$F(s) = \sqrt{\frac{1}{2N_s}\sum_{v=1}^{2N_s} F_s^2(v)} \quad (2)$$

If the data are correlated according to a long-range power-law, the fluctuation functions should increase by a power-law: $F(s) \propto s^{\alpha}$, where the slope of the line relating $\log F(s)$ and $\log s$ is the scaling

exponent α, which in turn quantifies the decay of the autocorrelation function.

2.3. Multiscale entropy analysis

A process with LRTC is likely exhibit complex structure on multiple time scale (Bhattacharya et al., 2005). Thus, we applied a recently developed measure, called multiscale entropy (Costa et al., 2002), to achieve a quantification of the signal complexity considering several time scales. It is based on the computation of the SampEn on coarse-grained sequences, which represents the system dynamics on different time scales. The SampEn has the positive aspect that it is independent of the sequence length and robust to noise data sets (Richman and Moorman, 2000).

Formally, given a one-dimensional discrete time series $\{x(i): i = 1, 2, \ldots, N\}$, first we construct the coarse-grained time series determined by the time scale factor τ as follows:

$$y_\tau(i) = \frac{1}{\tau} \sum_{i=(j-1)\tau+1}^{j\tau} x(i), \quad 1 \le j \le \frac{N}{\tau} = N_\tau \tag{3}$$

Once the coarse-grained time series are built, we calculate their SampEn, which assigns a non-negative value to each coarse-grained sequence. For the detailed description of SampEn, please refer to Richman's paper (Richman and Moorman, 2000). Two parameters including the embedding dimension m and the effective filter r, are necessary for the computation of SampEn. As in previous study (Zhang et al., 2007), we choose $m = 2$ and $r = 0.2\sigma$, where the σ is the standard deviation of the original sequence. The maximum analyzed time scales was 20.

The MSE curves can be used to compare qualitatively the signal complexity of different time series. Thus, a completely independent random sequence monotonically decreases with the scale factor, since it contains information only on the smallest time scale. In contrast, a fractal or long-range correlated sequence is relatively steady across scales (Costa et al., 2005b).

2.4. Surrogate data testing

Whether the power-law relationship reflects a true LRTC was tested by simply shuffling the original RSNA sequence to create surrogate data (Bhattacharya et al., 2005). The shuffled sequence preserved the mean and variance of the original sequence, but lacked the correlations between the original RSNA sequence. The results were subsequently compared with the original sequence for both groups, respectively. If shuffling of RSNA sequences eliminates the power-law relationship, then it can be concluded that the original RSNA sequences were ordered and interdependent.

2.5. Statistics

All the data are expressed as the mean ± S.E.M. Data were analyzed using the unpaired Student's t-test and significant differences between the original and surrogate data as well as conscious group and the anesthetized group were taken when $P < 0.05$.

3. Results

Traces show representative section of original neurograms obtained from multifibre recordings of the RSNA made one Wistar rat in conscious state (Fig. 1a) and another in anesthetized state (Fig. 1b), both with a 1000 Hz sampling frequency and a 50 s sampling period. There was no significant difference between conscious and anesthetized states either in blood pressure

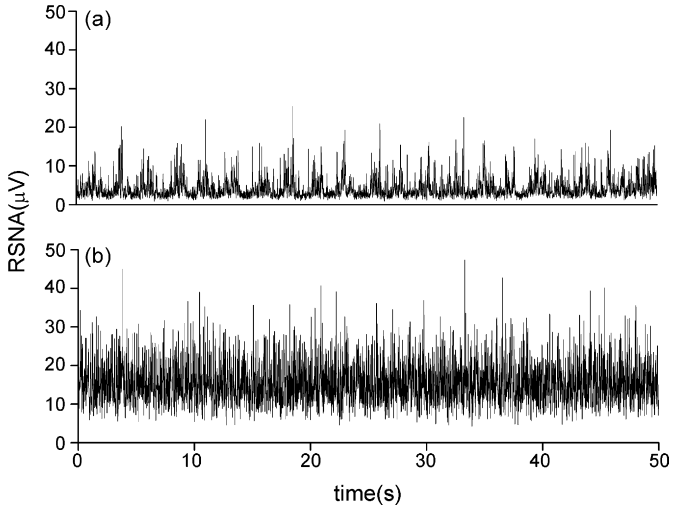

Fig. 1. (a) Representative section of original neurogram of RSNA from one Wistar rat in conscious state. (b) Representative section of original neurogram of RSNA from one Wistar rat in anesthetized state. The nerve signals were sampled by 1000 Hz.

(113 ± 4 mmHg vs. 100 ± 3 mmHg) or heart rate (461 ± 21 beats/min vs. 407 ± 14 beats/min).

3.1. Long-range temporal correlation as detected by DFA and MSE

It is well known that a time series was considered fractal in spite of the number of data and the length of the signals (Das et al., 2003). Fig. 2 showed the DFA and MSE analysis in conscious state between original and surrogate data. It can be seen that the scaling exponent of surrogate data was significantly lower than that of the original data (0.615 ± 0.018 vs. 0.502 ± 0.001, $P < 0.001$, $n = 15$, Fig. 2a). The entropy measure of RSNA from the original data increased over small time scales and then stabilized (from time scale 7) to a more or less constant value as the time scale increases. In contrast, the shuffled RSNA sequences decreased continuously on all the time scales (Fig. 2b). Furthermore, it was clear that the shuffled data produced less complex MSE values compared to those of the original data

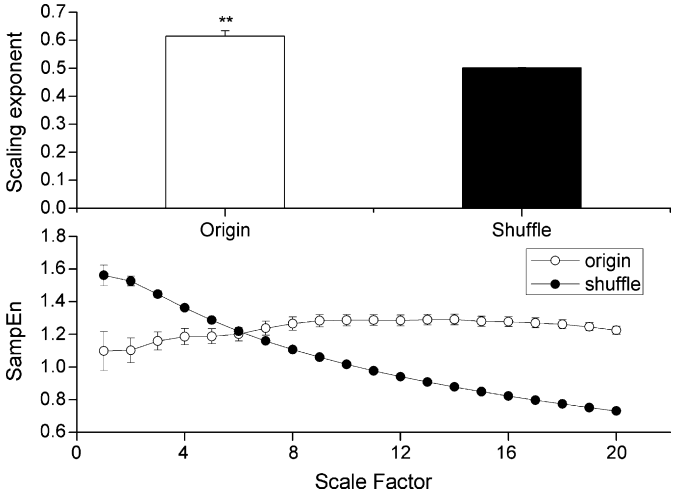

Fig. 2. DFA and MSE measurements of the multifibre RSNA obtained from Wistar rats between original and shuffled data in the conscious state. (a) Group values of scaling exponents α, in original data (open columns, 0.615 ± 0.018, $n = 15$) and shuffle data (filled columns, 0.502 ± 0.001, $n = 15$). $^{**}P < 0.01$, comparison between the original and shuffle data in conscious state. (b) The curve with open circle symbols represents the SampEn of original signals at time scales from 1 to 20, and the curve with filled circle symbols shows the SampEn of surrogate data at the same time scales.

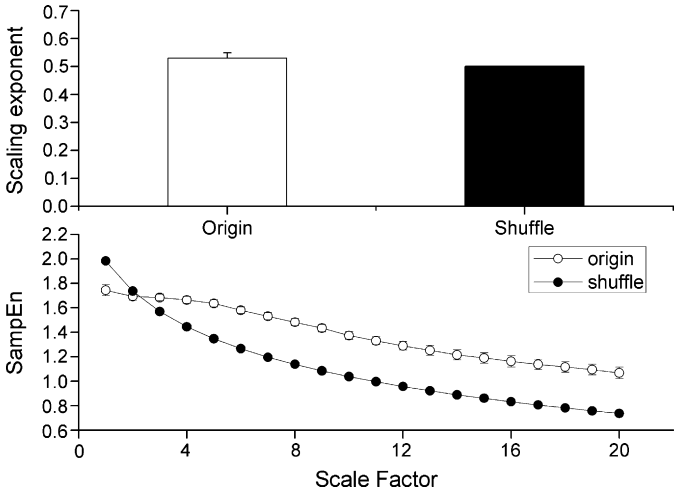

Fig. 3. DFA and MSE measurements of multifibre RSNA obtained from Wistar rats between original and shuffled data in the anesthetized state. (a) Group values of scaling exponents α, in original data (open columns, 0.530 ± 0.019, $n = 15$) and shuffle data (filled columns, 0.501 ± 0.001, $n = 15$). $P > 0.05$, comparison between the original and shuffle data in conscious state. (b) The curve with open circle symbols represented the entropy values of original signals at time scales from 1 to 20, and the curve with filled circle symbols showed the SampEn of surrogate data over the same time scales.

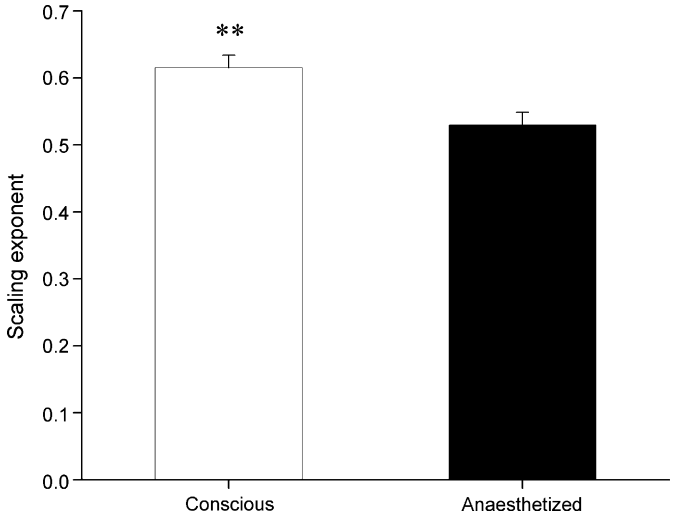

Fig. 4. Group values of scaling exponents α, in conscious rats (open columns, 0.615 ± 0.018, $n = 15$) and anesthetized rats (filled columns, 0.530 ± 0.019, $n = 15$). $^{**}P < 0.01$, comparison between the conscious group and the anesthetized group.

after time scales larger than 8 ($P < 0.05$). It was suggested that the MSE profiles for the shuffled sequence were qualitatively similar to that of an uncorrelated process. Thus both analyses (Fig. 2a and b) showed that the RSNA of conscious rats had a clear LRTC.

It can be seen that the entropy values of the original RSNA were significantly higher than that of the shuffled sequences from time scale 3, which indicated that the shuffled data produced less complex MSE values compared to that of the original data when the time scale was larger than 2 ($P < 0.001$, Fig. 3b). However, the entropy measure of the RSNA from both the original and shuffled data decreased continuously on all time scales, which indicated the LRTC in the anesthetized individuals was similar to that in the random process. For the results obtained from the DFA analysis of RSNA, there were no statistical differences between original and surrogate data in anesthetized state (0.530 ± 0.019 vs. 0.501 ± 0.001, $P = 0.512$, $n = 15$, Fig. 3a). The shuffled RSNA sequences only deviated to a small extent from the original scaling profiles.

3.2. Comparison of LRTC between conscious and anesthetized rats

Fig. 4 shows the group values of scaling exponent α obtained from both the conscious and anesthetized animals. It can be seen that the scaling exponent of the RSNA in conscious rats was significantly higher than that in anesthetized rats (0.615 ± 0.018 vs. 0.530 ± 0.019, $P = 0.007$, <0.01, $n = 15$), thus indicating the reduction of LRTC of the RSNA in the anesthetized state.

Fig. 5 illustrates the results of MSE analysis of the multifibre RSNA signals for both the conscious and anesthetized animal groups. Two different types of behavior were observed. One of them was that the entropy measure of RSNA, derived from the conscious group, increased over small time scales and then stabilized to a relatively constant value. On the other hand, the entropy measure for the time series derived from animals with anesthesia almost monotonically decreased, more or less similar to that of white noise (Costa et al., 2005b). For the scale one, which is the only scale considered by traditional single-scale-based "complexity" methods, the entropy assigned to the RSNA time series of the animals in the anesthetized state is much higher than the entropy assigned to the time series of animals in conscious state. By contrast, for sufficiently large time scales (in our particular case, this time scale is larger than 16, Fig. 5), the time series of RSNA from conscious rats were assigned the significant higher entropy values ($P < 0.05$). Thus, the MSE method indicates that dynamics in the conscious rats is more complex; contradicting the results obtained using the traditional SampEn algorithm.

4. Discussion

The intention of this study was twofold. Firstly, the issue was addressed as to whether the LRTC of multifibre RSNA, representing a nonlinear dynamical system with high-dimensionality and instability existed, and could be detected by DFA and MSE. Also, the issue of whether a power-law relationship reflects a true LRTC was examined by simply shuffling the original RSNA sequence to create surrogate data. Secondly, the hypothesis was tested that the pattern of RSNA, obtained from anesthetized animals with a mixture of chloralose and urethane, represented weakened LRTC compared to that in conscious rats.

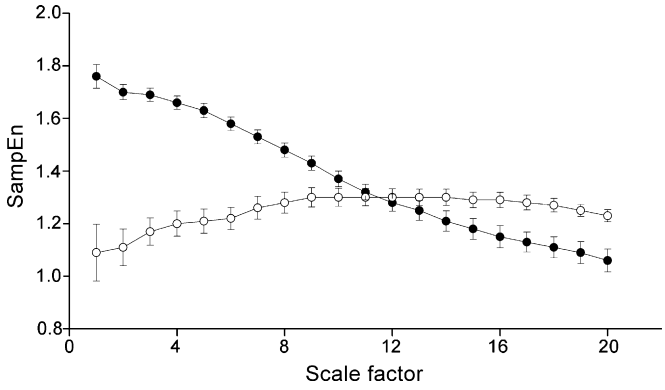

Fig. 5. MSE analysis of time series derived from RSNA of anesthetized and conscious rats. Symbols (open circle symbols for conscious rats and filled circle symbols for anesthetized rats, $n = 15$ for both groups) represent the mean values of SampEn for each group and the bars represent the standard error. Parameters to calculate SampEn are $m = 2$ and $r = 0.2\sigma$. Time series length is 164 s. The SampEn from conscious rats are significantly ($P < 0.05$) higher than that of anesthetized animals for time scales larger than 16.

A previous study (Bak et al., 1988) indicated that LRTC were built up through local interactions until they extend throughout the entire system. LRTC have been observed in a wide variety of complex phenomena (Stanley et al., 1994) including heartbeat intervals (Ashkenazy et al., 2001), DNA sequences (Peng et al., 1992), and gait patterns (Hausdorff et al., 1995). In neurophysiology, similar LRTC have been investigated from microscopic to macroscopic domains, ranging from medullary sympathetic neurons (Lewis et al., 2001) and to human brain oscillations (Linkenkaer-Hansen et al., 2001) to behavior performance, such as measuring the error associated with estimation of temporal/spatial intervals (Gilden et al., 1995), or long memory processes in human coordination (Chen et al., 1997). All the studies provide a strong argument that the scale-free temporal correlation is an intrinsic part of the overall neural information processing mechanism.

One of the most stimulating findings of the present investigation was a clear comparison of LRTC of the multifibre RSNA signals between the conscious and anesthetized animals. The fact that the scaling exponent of 0.615 in the conscious state decreased to 0.530 during anesthesia suggested that the underlying dynamics of RSNA time series tended to become much more stochastic. Furthermore, the MSE measure revealed that the RSNA had a complex structure and exhibited the presence of LRTC, which has been associated with complex physiological systems (Goldberger et al., 2002). Goldberger et al. (1996) suggested that LRTC represented the time-scale-invariant behavior might prevent excessive mode locking, which would restrict the functional responsiveness of the organism to unexpected challenges. Thus, our results were consistent with the fact that the rats after being anesthetized had a weakened ability to respond to the changes in the environment or external perturbations compared to that of conscious animals. A previous study has postulated that the fractal component of heart rate variability (HRV) in healthy humans arose from an interaction between cardiac sympathetic and vagal outflows at the sinoatrial node (Goldberger et al., 1996). Thus, our data might play an important role in explaining the fractal exponents of HRV, since the RSNA contains cardiac-related activity. However, it remains to be investigated whether the effect of anesthesia on LRTC properties of RSNA has play a role in changing the fractal component of HRV.

In summary, this study shows that the analyses of DFA and MSE can be applied to measure LRTC in multifibre RSNA signals. Our results demonstrate that DFA can provide a simple quantitative parameter to represent the characterization of LRTC embedded in non-stationary time series, such as RSNA signals. The MSE measure revealed the RSNA complex structure and showed the presence of LRTC associated with complex physiological system. The time-scale-invariant behavior represents a form of memory, in that the current values of the RSNA is determined not only by recent events, but also by the those in the distant past. In contrast, such memory is absent for a uncorrelated random process. Thus, the results demonstrate that apparently random fluctuations in the RSNA are dictated by a complex deterministic process that imparts "long-term" memory to the dynamic system. However, this memory is significantly weakened by anesthesia.

Acknowledgements

This work was supported by grants from the NBRPC (2007CB914803) and the NSFC (30470453 and 30640037).

References

Ashkenazy Y, Ivanov PC, Havlin S, Peng CK, Goldberger AL, Stanley HE. Magnitude and sign correlations in heartbeat fluctuations. Phys Rev Lett 2001;86:1900.
Bak P, Tang C, Wiesenfeld K. Self-organized criticality. Phys Rev A 1988;38:364.
Bhattacharya J, Edwards J, Mamelak AN, Schuman EM. Long-range temporal correlations in the spontaneous spiking of neurons in the hippocampal–amygdala complex of humans. Neuroscience 2005;131:547–55.
Bornas X, Llabres J, Noguera M, Lopez AM, Gelabert JM, Vila I. Fear induced complexity loss in the electrocardiogram of flight phobics: a multiscale entropy analysis. Biol Psychol 2006;73:272–9.
Bunde A, Havlin S, Kantelhardt JW, Penzel T, Peter J-H, Voigt K. Correlated and uncorrelated regions in heart-rate fluctuations during sleep. Phys Rev Lett 2000;85:3736.
Burgess DE, Zimmerman TA, Wise MT, Li S-G, Randall DC, Brown DR. Low-frequency renal sympathetic nerve activity, arterial BP, stationary "1/f noise", and the baroreflex. Am J Physiol 1999;277:R894–903.
Chen Y, Ding M, Kelso JAS. Long memory processes (1/fâlpha Type) in human coordination. Phys Rev Lett 1997;79:4501.
Costa M, Goldberger AL, Peng CK. Multiscale entropy analysis of complex physiologic time series. Phys Rev Lett 2002;89:068102.
Costa M, Goldberger AL, Peng CK. Broken asymmetry of the human heartbeat: loss of time irreversibility in aging and disease. Phys Rev Lett 2005a;95:198102.
Costa M, Goldberger AL, Peng CK. Multiscale entropy analysis of biological signals. Phys Rev E 2005b;71:021906.
Das M, Gebber GL, Barman SM, Lewis CD. Fractal properties of sympathetic nerve discharge. J Neurophysiol 2003;89:833–40.
DiBona GF, Jones SY. Dynamic analysis of renal nerve activity responses to baroreceptor denervation in hypertensive rats. Hypertension 2001;37:1153–63.
DiBona GF, Jones SY, Sawin LL. Chaotic behavior of renal sympathetic nerve activity: effect of baroreceptor denervation and cardiac failure. Am J Physiol Renal Physiol 2000;279:F491–501.
Escudero J, Abasolo D, Hornero R, Espino P, Lopez M. Analysis of electroencephalograms in Alzheimer's disease patients with multiscale entropy. Physiol Meas 2006;27:1091–106.
Gifani P, Rabiee HR, Hashemi MH, Taslimi P, Ghanbari M. Optimal fractal-scaling analysis of human EEG dynamic for depth of anesthesia quantification. J Franklin Inst 2007;344:212–29.
Gilden DL, Thornton T, Mallon MW. 1/f noise in human cognition. Science 1995;267:1837–9.
Goldberger AL, Peng C-K, Hausdorff J, Mietus J, Havlin S, Stanley HE. Fractals and the heart. In: Iannaconne PM, Khokha M, editors. Fractal Geometry in Biological Systems: An Analytical Approach. Boca Raton, FL: CRC; 1996. p. 249–66.
Goldberger AL, Peng CK, Lipsitz LA. What is physiologic complexity and how does it change with aging and disease? Neurobiol Aging 2002;23:23–6.
Hausdorff JM, Peng CK, Ladin Z, Wei JY, Goldberger AL. Is walking a random walk? Evidence for long-range correlations in stride interval of human gait. J Appl Physiol 1995;78:349–58.
Huang C, Yoshimoto M, Miki K, Johns EJ. The contribution of brain angiotensin II to the baroreflex regulation of renal sympathetic nerve activity in conscious normotensive and hypertensive rats. J Physiol (London) 2006;574:597–604.
Iriki M, Kozawa E. Renal sympathetic baroreflex during normoxia and during hypoxia in conscious and in anesthetized rabbits. Pflugers Arch 1983;398:23–6.
Kantelhardt JW, Koscielny-Bunde E, Rego HHA, Havlin S, Bunde A. Detecting long-range correlations with detrended fluctuation analysis. Physica A 2001;295:441–54.
Lewis CD, Gebber GL, Larsen PD, Barman SM. Long-term correlations in the spike trains of medullary sympathetic neurons. J Neurophysiol 2001;85:1614–22.
Li D, Jin YX, Yang Z, Zhang T. Analysis of multifibre renal sympathetic nerve recordings. Lect Notes Comput Sci 2006;3973:734–9.
Linkenkaer-Hansen K, Nikouline VV, Palva JM, Ilmoniemi RJ. Long-range temporal correlations and scaling behavior in human brain oscillations. J Neurosci 2001;21:1370–7.
Malpas SC. The rhythmicity of sympathetic nerve activity. Prog Neurobiol 1998;56:65–96.
Malpas SC, Evans RG, Head GA, Lukoshkova EV. Contribution of renal nerves to renal blood flow variability during hemorrhage. Am J Physiol 1998;274:R1283–94.
Malpas SC, Ninomiya I. A new approach to analysis of synchronized sympathetic nerve activity. Am J Physiol 1992;263:H1311–7.
Matsukawa K, Ninomiya I. Anesthetic effects on tonic and reflex renal sympathetic nerve activity in awake cats. Am J Physiol 1989;256:R371–8.
Morita H, Nishida Y, Uemura N, Hosomi H. Effect of pentobarbital anesthesia on renal sympathetic nerve activity in the rabbit. J Auton Nerv Syst 1987;20:57–64.
Nikulin VV, Brismar T. Long-range temporal correlations in electroencephalographic oscillations: relation to topography, frequency band, age and gender. Neuroscience 2005;130:549–58.
Parish LM, Worrell GA, Cranstoun SD, Stead SM, Pennell P, Litt B. Long-range temporal correlations in epileptogenic and non-epileptogenic human hippocampus. Neuroscience 2004;125:1069–76.
Peng CK, Buldyrev SV, Goldberger AL, Havlin S, Sciortino F, Simons M, et al. Long-range correlations in nucleotide sequences. Nature 1992;356:168–70.
Persson PB, Stauss H, Chung O, Wittmann U, Unger T. Spectrum analysis of sympathetic nerve activity and blood pressure in conscious rats. Am J Physiol 1992;263:H1348–55.
Richman J, Moorman J. Physiological time-series analysis using approximate entropy and sample entropy. Am J Physiol 2000;278:H2039–49.
Stanley HE, Buldyrev SV, Goldberger AL, Goldberger ZD, Havlin S, Mantegna RN, et al. Statistical mechanics in biology: how ubiquitous are long-range correlations? Physica A 1994;205:214–53.

Stauss HM, Persson PB, Johnson AK, Kregel KC. Frequency–response characteristics of autonomic nervous system function in conscious rats. Am J Physiol 1997;273:H786–95.

Trzebski A, Smietanowski M, Zebrowski J. Repetitive apneas reduce nonlinear dynamical complexity of the human cardiovascular control system. J Physiol Pharmacol 2001;52:3–19.

Yang Z, Zhang T, Coote JH. Synchrony analysis between blood pressure and sympathetic nerve signal inhibited by atrial receptor stimulation in Wistar rats. Exp Physiol 2002;87:461–8.

Zhang T, Huang C, Johns EJ. Neural regulation of kidney function by the somatosensory system in normotensive and hypertensive rats. Am J Psychol 1997;273:R1749–57.

Zhang T, Johns E. Chaotic characteristic of renal nerve peak interval sequence in normotensive and hypertensive rats. Clin Exp Pharmacol Physiol 1998;25: 896–903.

Zhang T, Yang Z, Coote JH. Autonomic neuroscience: cross-sample entropy statistic as a measure of complexity and regularity of renal sympathetic nerve activity in the rat. Exp Physiol 2007;92:659–69.